MICRO PULSE LIDAR MEASUREMENTS FOR POLAR STRATOSPHERIC CLOUD MONITORING IN COASTAL ANTARCTICA. I. DEPOLARIZATION RATIO COMPARISON WITH CALIOP

C. Córdoba-Jabonero[1], J.L. Guerrero-Rascado[2,3], D. Toledo[1], M. Parrondo[1], M. Yela[1], M. Gil[1], H. Ochoa[4]

[1]Instituto Nacional de Técnica Aeroespacial (INTA), Atmospheric Research and Instrumentation Branch, Torrejón de Ardoz, 28850, Madrid (Spain), cordobajc@inta.es

[2]Andalusian Center for Environmental Research (CEAMA), University of Granada - Autonomous Government of Andalusia, Granada (Spain)

[3]Department of Applied Physics, University of Granada, Granada (Spain)

[4]Dirección Nacional del Antártico (DNA), Buenos Aires (Argentina)

ABSTRACT

Polar Stratospheric Clouds (PSCs) play a determinant role in the polar ozone depletion, indicating the importance of the PSC characterization.

Both lidar parameters -the backscattering (R) and volume depolarization (δ) ratios- are usually used for PSC detection and identification. In this work, an improved version of the standard NASA/Micro Pulse Lidar (MPL-4), which includes a built-in depolarization module, has been used for PSC observations over the coastal Antarctic Belgrano II station (Argentina, 77.9ºS 34.6ºW). Examination of the MPL-4 δ parameter as a suitable index for PSC-type discrimination is based on the analysis of the two-channel data, i.e. both parallel (p-) and perpendicular (s-) MPL signals. This study focuses on the comparison of the δ-profiles as obtained from MPL-4 measurements with those reported from the space-borne lidar CALIOP to test the degree of agreement.

Results indicate that there is a good correlation between both depolarization profiles once MPL-4 calibrated depolarization parameters are calculated. This correlation is based on the height range of the layered structure as well as the δ values found for each layer. As expected, this agreement is much better when the CALIPSO ground-track overpass is much closer to Belgrano II station.

1. INTRODUCTION

The polar stratosphere in both hemispheres is characterized by very low temperatures during winter leading to the formation of Polar Stratospheric Clouds (PSC). As it is known, they have an important role in polar ozone depletion by activating compounds such as chlorine and other halogenated species through heterogeneous chemistry processes occurring on their surfaces [1].

In particular, Antarctic temperatures can reach rather lower values than Arctic temperatures below their threshold for PSC formation [2], favoring a higher occurrence of PSCs over the Antarctic continent, including ice PSCs. In this way, extensive Antarctic PSC lidar studies have been reported to date by five Antarctic stations: South Pole/Amundsen-Scott (USA, 89.98ºS 24.8ºE, 2835 m asl) [3], McMurdo (USA, 78.0ºS 167.0ºE) [4, 5], Syowa (Japan, 69.0ºS 39.5ºE) [6], Davis (Australia, 68.6ºS 78.0ºE) [7], and Dumont d'Urville (France, 66.4ºS 140.0ºE) [8]. In addition, the space-borne lidar CALIOP on board of CALIPSO (Cloud-Aerosol Lidar and Infrared Pathfinder Satellite Observation, www-calipso.larc.nasa.gov) provides PSC valuable information from 2006 at regional scale on both poles [9].

An improved version of the standard NASA/Micro Pulse Lidar (MPL v.4, MPL-4, Sigma Space Corp.), which includes a built-in depolarization module, is currently used for PSC observations in the Antarctic Belgrano II station (Argentina, 77.9ºS 34.6ºW, 256 m asl) from 2009. This station remains well inside the polar vortex during wintertime [2] providing an excellent location for PSC observations. Therefore, one more ground-based station is added to those devoted to long-term PSC measurements. Older versions than MPL-4 were already deployed in two of those five Antarctic stations: Syowa (Japan) and South Pole/ Amundsen-Scott (USA), but any of them include polarization measuring capabilities similar to the MPL-4 ones.

The different degree of depolarization in terms of linear volume depolarization ratio (δ) together with the observed backscattering ratio (total backscatter-to-molecular coefficient ratio) allows for a qualitative PSC-type discrimination [i.e., 5, 9]. Indeed, this PSC-type identification is critical on polar ozone depletion research, and directly linked to the stratospheric temperature variability.

A good performance of the MPL-4 system on PSC detection was previously achieved in the Arctic [10] with some limitations related in fact to the depolarization measurements. Therefore, this particular MPL-4 depolarization feature, that is the δ parameter

estimation from MPL-4 measurements, is examined in this work. Then, MPL-4 depolarization retrievals are analyzed in comparison with the PSC depolarization ratio reported from the space-borne lidar CALIOP to test the degree of agreement.

2. METHODS

2.1 Lidar systems

2.1.1 Ground-based lidar: MPL-4

The MPL-4 lidar is an improved version of the standard Micro Pulse Lidar (MPL-3) in routine operation within the NASA/MPLNET (Micro-Pulse Lidar Network, http://mplnet.gsfc.nasa.gov). The MPL-4 system [11] is configured in a zenith monostatic coaxial alignment and is based on an eye-safe pulsed Nd:YLF laser emitting at 527 nm with a high repetition-rate (2500 Hz) and low-energy (10 μJ). Its receiver system consists of a Maksutov-Cassegrain 18 cm-diameter telescope, a birefrigent polarizer cell, and an avalanche photodiode detector. Backscattered signals are registered at 1-min integrated time and 75-m vertical resolution, commuting at each time the polarization module from parallel- to perpendicular-polarized detection (p- and s-channels, respectively). The system is able to probe the atmosphere up to 30 km with a good enough signal-to-noise ratio, and the full overlap is achieved at altitudes around 4 km. The MPL-4 system is small, easy-handle with high autonomy and operational in full-time continuous mode. Hourly averaged profiles are then analyzed to study the spatial and temporal variability of the PSC distribution.

2.1.2 Satellite-based lidar: CALIOP

The CALIPSO satellite carries aboard the first satellite-borne lidar instrument CALIOP (Cloud-Aerosol Lidar with Orthogonal Polarization) which provides horizontally- (along the CALIPSO track) and vertically-resolved measurements for aerosol and clouds distributions at a global scale. CALIOP is based on diode-pumped Nd:YAG lasers emitting linearly polarized pulses with a repetition rate of 20.16 Hz and a pulse length of ~ 20 ns, energy per pulse of 220 mJ at 1064 nm and ~ 110 mJ at 532 nm. Its receiver system consist of a 1m-diameter telescope which feeds a three-channel receiver measuring the backscattered intensity at 1064 nm and the two orthogonal polarization components at 532 nm (parallel and perpendicular). A full description of the CALIOP system can be found in [12] and [13]. CALIOP provides data at 532 nm (the closest wavelength to that of the MPL-4 system) with a different vertical resolution as a function of altitude: 30 m at < 8.2 km, 60 m at 8.2-20.2 km, 180 m at 20.2-30.1 km, and 300 m at 30.1-40.0 km. In order to improve the signal-to-noise ratio, a horizontal averaging over 5 km CALIPSO ground-track and a vertical 7-point adjacent averaging are applied.

2.2 Depolarization data processing

Several definitions are available in the lidar community to describe the depolarization phenomena caused by atmospheric constituents. A review of the most common parameters used in lidar literature is given by [14].

2.2.1 Ground-based depolarization measurements

From the practical point of view, the most general expression to calculate the linear volume depolarization ratio is:

$$\delta(z) = K\frac{P^{\perp}(z)}{P^{\parallel}(z)} + \chi \qquad (1)$$

where $P^{\perp}(z)$ and $P^{\parallel}(z)$ are the s- and p-components of the measured MPL signals, respectively, once corrected for intrinsic instrumental factors [11]; K is a calibration constant that accounts for the differences of the receiver channel gains; and χ is a correction to account for any slight mismatch in the transmitter and detector polarization planes and any impurity of the laser polarization state [15, 16]. Optimal K and χ values are obtained by using fitting procedures with molecular backgrounds.

2.2.2 Satellite-based depolarization measurements

CALIPSO provides Level 1 and Level 2 products [17]. The Level 1 products include lidar calibrated and geo-located profiles of attenuated-backscatter coefficient at 1064 nm, and total and perpendicular-polarized attenuated backscatter coefficient at 532 nm. The Level 2 products include cloud layer, aerosol layer and aerosol profiles at different horizontal resolutions.

The Level 1 V3-01 (version 3.01, validated stage 1) attenuated-backscatter profile products at 532 nm (total and perpendicular-polarized) are used in this study. The attenuated-backscatter coefficient profile is defined as the volume backscatter coefficient β multiplied by the two-way atmospheric transmission T^2 [18]. On the other hand, the linear total depolarization ratio δ_{total} is defined as:

$$\delta_{total}(z) = \frac{\beta^{\perp}(z)}{\beta^{total}(z)} \qquad (2)$$

being $\beta^{total}=\beta^{\perp}+\beta^{\parallel}$, where $\beta^{\perp}(z)$ and $\beta^{\parallel}(z)$ are the global (particles and molecules) backscatter coefficient for s- and p-polarized components, respectively, and z is the range. For convenience, Eq. 2 can be multiplied by the term T^2, allowing for expressing the linear total depolarization ratio δ_{total} in terms of attenuated-backscatter coefficients:

$$\delta_{total}(z) = \frac{\beta^{\perp}(z)}{\beta^{total}(z)} = \frac{\beta^{\perp}(z)\cdot \mathrm{T}^2}{\beta^{total}(z)\cdot \mathrm{T}^2} = \frac{\beta_{att}{}^{\perp}(z)}{\beta_{att}{}^{total}(z)} \quad (3)$$

being $\beta_{att}{}^{total}=\beta_{att}{}^{\perp}+\beta_{att}{}^{\parallel}$, where $\beta_{att}{}^{\perp}(z)$ and $\beta_{att}{}^{\parallel}(z)$ are the attenuated-backscatter coefficient for s- and p-polarized components, respectively. $\beta_{att}{}^{\perp}$ and $\beta_{att}{}^{total}$ are provided by the CALIPSO Level 1 products. Finally, the δ_{total} values are converted into δ values using the following relationship [14]:

$$\delta(z) = \frac{\delta_{total}(z)}{1-\delta_{total}(z)} \quad (4)$$

Therefore, the linear volume depolarization ratio δ can be compared between MPL-4 and CALIPSO data.

3. RESULTS AND DISCUSSION

During the 2009, 2010 and 2011 Antarctic winters, a total of 189 CALIPSO overpasses nearby the Belgrano II station (distance criteria between the satellite ground-track and the station less 50 km) were carried out. Among them, 104 overpasses are coincident with MPL-4 measurements reporting PSC detection. In this work, three cases, one for each year, of the comparison of MPL-4 to CALIPSO data for PSC depolarization assessment are shown in Figures 1-3 (see Figure captions for more detail), respectively.

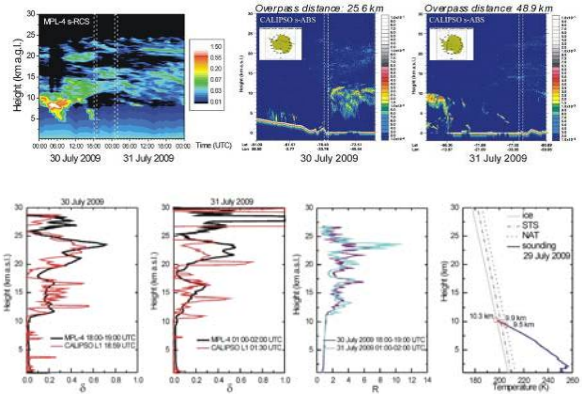

Figure 1. Top panels: Daily time evolution of MPL-4 range-corrected s-signal (s-RCS, a.u.), where white dashed lines indicate coincidence in time with CALIPSO overpass above Belgrano II station. CALIPSO s-attenuated-backscatter coeff. (s-ABS, $km^{-1}sr^{-1}$) along the ground-track (white dashed lines indicate CALIPSO overpass coincidence above the Belgrano II station). Inside figure-map: CALIPSO ground-track over Antarctica (Belgrano II location is indicated by a yellow star). Bottom panels: MPL-4 and CALIPSO δ-profiles comparison and MPL-4 R-profiles at the nearest CALIPSO overpass distance from Belgrano II station (as shown by those shaded white lines). Temperature radiosounding, closest in time to lidar measurements.

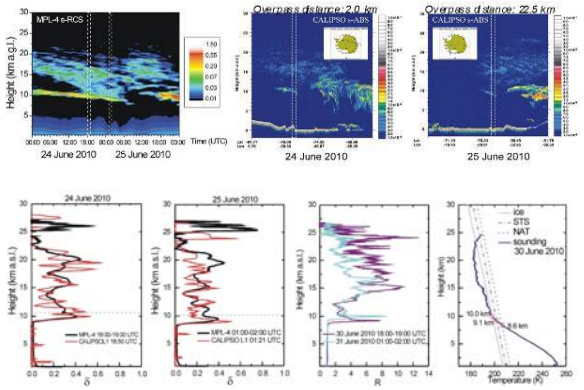

Figure 2. The same as Fig. 1, but on 24-25 June 2010.

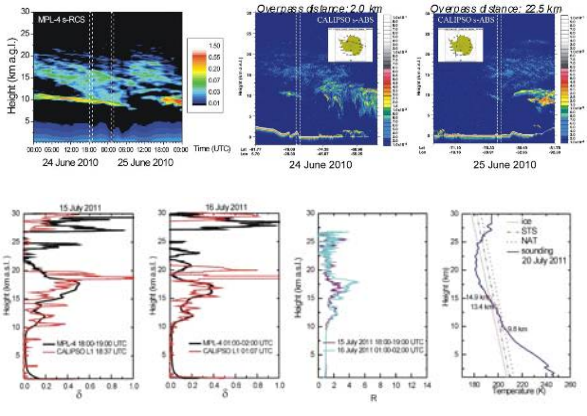

Figure 3. The same as Fig. 1, but on 15-16 July 2011.

PSC distribution and other features as observed over Belgrano II on these days (see Figures 1-3) is described next.

3.1 30-31 July 2009 case (see Figure 1)

MPL-4 data show PSCs from 10 km up to 28.5 km (high variability) together with cirrus clouds (CC) preventing PSC detection in the interval 04:00 - 08:00 UTC on 30 July. Next day, PSC presence is quite stable along all the day and an isolated and relatively thin CC is observed until around 08:00 UTC. Three PSC layers are well differentiated. CALIPSO data indicate PSCs above 11.5 km and tropospheric clouds below that height over the ocean are present on 30 July. During the overpass (18:59 UTC), strong lidar returns above 11.5 km are identified as PSCs. Next day, PSCs are detected above 10 km height over Antarctica. The comparison of those results presents a good correlation on 30 July, since similar δ-layering (3 layers) and δ values for each layer are found. A poorer δ-profile agreement is found on 31 July, although a similar layering is still observed.

3.2 24-25 June 2010 case (Figure 2)

On 24 June, a persistent CC 1-km thick layer is found, descending from around 10.5 km height (at the beginning of the day) down to 9.5 km (at the end) from MPL4 data. A well-defined PSC 6-km thick layer was evolving and vertically spreading along the day, coupling finally with a CC later at 16:00 UTC. Next day, PSCs almost permanently are observed at altitudes higher than 10 km height. CCs are present until 09:00 UTC and after 11:00 UTC. From CALIPSO data, strong lidar returns are coming from a layer at 9.5-10.5 km height, with additional stratospheric features above. Thus, an excellent correlation between MPL-4 and CALIPSO δ-profiles is found on 24 June, with similar layering and values. Next day, δ profiles are comparable in layering structure and values for both PSCs and CCs despite the upper δ layer was underestimated by CALIPSO in around 1.6 km. Therefore, a good agreement regarding the type of scatterers (PSC vs. CC) is found.

3.3 15-16 July 2011 case (Figure 3)

From MPL-4data on 15 July, PSCs are found from 10 up to 30 km height together with an isolated CC from 11:00 to 17:00 UTC between 8.5 and 10 km height. Next day, PSC presence is more stable, although PSC detection is limited by low thick cloud screening from 10:00 UTC on. CALIPSO data show strong lidar returns above 10 km height, which are identified as PSCs during the overpass on this day, while on 16 July PSCs are detected between 11 and 20 km height over areas surrounding the Belgrano II station. A poorer δ-profile agreement is found in this case due to larger distances between the CALIPSO ground-track overpass and Belgrano II station.

4. CONCLUSIONS

This preliminary study represents the first application of lidar depolarization technique to Antarctic PSC detection and identification by using an improved version (MPL-4) of the standard NASA/Micro Pulse Lidar. MPL-4 depolarization profiles obtained during the 2009-2011 Austral winters over Belgrano II station (Antarctica) were compared with CALIPSO data as a reference. A few examples have been shown in this work to illustrate such a comparison analysis. Results indicate a good correlation between both ground- and space-based lidar datasets once MPL-4 calibrated depolarization parameters are applied. As expected, this agreement is much better when the CALIPSO ground-track overpass is much closer to the Belgrano II station.

ACKNOWLEDGMENTS

This work is supported by the Spanish Ministry for Research and Innovation (MICINN) under grant CGL2010-20353 (project VIOLIN). CALIPSO data were obtained from the NASA Langley Research Center Atmospheric Science Data Center. Authors specially thank the DNA/IAA team at Belgrano II station for their valuable assistance and support.

REFERENCES

1. Solomon, 1999: *Rev.Geophys.,* **37**, 275-316.
2. Parrondo *et al.,* 2007: *Atmos. Chem. Phys.,* **7**, 1-7.
3. Campbell and Sassen, 2008: *J. Geophys. Res.,* **113**, D20204, doi:10.1029/2007JD009680.
4. Adriani *et al.,* 2004: *J. Geophys. Res.,* **109**, D24211, doi:10.1029/2004JD004800.
5. Maturilli *et al.,* 2005: *Atmos. Chem. Phys.,* **5**, 2081-2090.
6. Shibata *et al.,* 2003: *J. Geophys. Res.,* **108**, D3, 4105, doi:10.1029/2002JD002713.
7. Innis and Klekociuk, 2006: *J. Geophys. Res.,* **111**, D22102, doi:10.1029/2006JD007629.
8. Santacesaria *et al.,* 2001: *Tellus,* **53B**, 306-321.
9. Pitts *et al.,* 2009: *Atmos. Chem. Phys*., **9**, 7577-7589.
10. Córdoba-Jabonero *et al.,* 2009: *J. Atmos. Ocean. Technol.,* **26**, 2136-2148.
11. Campbell *et al.,* 2002: *J. Atmos. Ocean. Technol*., **19**, 431-442.
12. Winker *et al.,* 2007: *Geophys. Res. Lett*., **34**, L19803, doi:10.1029/2007GL030135.
13. Hunt *et al.,* 2009: *J. Atmos. Ocean. Technol*., **26**, 1214-1228.
14. Cairo *et al.,* 1999: *Appl. Opt*., **38**, 4425-4432.
15. Sassen and Benson, 2001: *J. Atmos. Sci*., **58**, 2103-2112.
16. Sassen, 2005: Polarization in Lidar, in *Lidar: Range-Resolved Optical Remote Sensing of the Atmosphere,* Ed. C. Weitkamp, Springer Ser., Singapore.
17. Powell *et al.,* 2010: Data Management System, Data Products Catalog, in *Cloud-Aerosol LIDAR Infrared Pathfinder Satellite Observations,* Doc. No: PC-SCI-503, NASA Langley Research Center, Virginia, USA.
18. Hostetler *et al.,* 2006: Calibration and level 1 data products, in *CALIOP algorithm theoretical basis document,* Doc. No: PC-SCI-201, NASA Langley Research Center, Hampton, Virginia, USA.